Batteries & Supercaps

Research Article
doi.org/10.1002/batt.202200436

Chemistry Europe
European Chemical Societies Publishing

www.batteries-supercaps.org

Special Collection

Adjusting the Electrolyte Polarity to Address the Dissolution Issue of Organic Electrode

Zitong Liu,[c] Ting Xu,[c] Xianjiao Meng,[c] Yali Zhao,[c] Qing Lan,[c] Yutao Liu,[c] Zhiping Song,[c] Jian Qin,[c] and Hui Zhan*[a, b]

Small organic molecules with carbonyl active site are a prominent member in the family of organic electrode material, due to the reversible reaction and more tunable electrochemical property. However, the dissolution loss is the biggest obstacle in its application. In this work, we tried to address the dissolution issue of 5,7,12,14-pentacenetetrone (PT), a typical quinone-based organic electrode. Highly concentrated electrolyte of 5 M LiTFSI DME was used and it significantly reduced the dissolution and well maintained the capacity after 500 cycles. Besides, through the investigation of the relationship between solvent/electrolyte property and dissolution, and the interaction between electrode and electrolyte, a guiding rule of the dependence of dissolution on polarity was proposed. With the rule, non-polar solvent of hexane was further added as co-solvent and its-adding decreased the polarity and substantially eliminated the dissolution loss. The work supplies a common electrolyte strategy to address the dissolution issue of small organic molecules.

Introduction

Lithium-ion batteries have been widely used because of their high energy density, high operating voltage and many other advantages.[1] However, commercial lithium-ion battery relies entirely on the intercalation inorganics, and it generates the concerns on environment problems, resource consumption as well as cost.[2] In addition, the capacity of traditional intercalated-inorganics is severely limited by the crystalline structure.[3,4] Comparatively, organic electrode materials (OEM) are mainly composed of hydrocarbons, oxygen, nitrogen, sulfur and other elements that are abundant in nature. Moreover, the molecular structure of organic materials can be designed and tailored according to voltage and capacity requirements. The sustainability and cost-effective merits make OEM a good substitute for inorganic electrodes in the upcoming battery innovation.[5–7]

Among the OEM family, carbonyl compounds are a prominent role due to its highly reversible reaction, good compatibility and molecular tunability. The core moiety of compounds is the carbonyl group, its N-type reaction endows it with electron-accepting capability. The smallest active carbonyl organics of $Li_2C_6O_6$ was first proposed in 2008,[8] and it had as high as >800 mAh/g capacity if 6 electrons being injected, however, the solubility and increasing barrier along with electron-gain much harmed its stability, hence it had to be cycled within restricted voltage range. Hereafter, many other carbonyl organics or polymers were proposed and synthesized, and it was widely proved and accepted that the carbonyl organics with more repeating unit and even polymer with carbonyl moiety could better maintain the capacity. For instance, C_4Q presented enhanced cycling stability than quinone,[9,10] and poly(anthraquinone sulfide) could achieve undecayed capacity in thousands of cycles.[11,12] Though using polymers electrode could tackle the stability problem at the source, the necessary but redundant bridged-bond reduced the capacity, and the repeating unit complicated the spatial configuration and brought limited room to molecule-structure adjustment. With this scenario, attentions were turned back to small organic molecules in the recent years and many efforts was devoted to its stability improvement.

Typical approaches included introducing function group and material processing. For example, DMAQ was obtained by introducing two methoxy groups into AQ, and lower solubility in ether-like electrolytes was observed.[13] It was explained by the larger conjugate plane and increased interaction between molecules. Similarly, strong polar moieties of $-SO_3M$ was added into the indigo molecule and the obtained derivatives showed excellent cycling stability.[14] On the other hand, Park combined photoflavonoids (LF) and single-walled carbon nanotubes (SWNTs) to immobilize the active substance by virtue of strong physical adsorption between them.[15] The team then grafted DANQ onto the fluid-collecting surface using a chemical modification and it effectively prevented the volume decay.[16]

[a] Prof. H. Zhan
Hubei Key Lab of Electrochemical Power Sources, College of Chemistry and Molecular Science
Wuhan University
Wuhan 430072, China
E-mail: zhanhui3620@126.com
[b] Prof. H. Zhan
Engineering Research Center of Organosilicon Compounds & Materials, Ministry of Education
Wuhan University
Wuhan 430072, China
[c] Z. Liu, T. Xu, X. Meng, Dr. Y. Zhao, Dr. Q. Lan, Dr. Y. Liu, Prof. Z. Song, Dr. J. Qin
Hubei Key Lab of Electrochemical Power Sources
Wuhan University
Wuhan 430072, China

Supporting information for this article is available on the WWW under https://doi.org/10.1002/batt.202200436

Special Collection An invited contribution to a Special Collection on Organic Batteries

Research Article
doi.org/10.1002/batt.202200436
Chemistry Europe
European Chemical Societies Publishing

Though the organic electrode material and insoluble matrix can be composite anchored, the complex processing as well as the limited number of energy species on the substrate cannot be ignored. In addition, enhancing the π-π intermolecular interaction between materials[17,18] or forming intramolecular hydrogen bond[19,20] by designing molecular structures are also effective strategies to achieve stable cycling of organic electrode materials.

As solubilization involves the interaction between electrolyte and small organic molecules, the dissolution issue can also be targeted by the electrolyte modification. Actually, it was a recent focus and some studies proved its effectiveness. For instance, ionic liquid electrolyte and concentrated electrolyte could enable thousands of stable cycling of PTCDA.[21,22] Polymer electrolytes[23,24] also contributed to the stable cycling of carbonyl organics. Though with significant progress, we had to notice that these efforts were aimed to relatively bigger molecules which was intrinsically less beset by the dissolution loss. Additionally, guiding principles was still lacking and thus rationally pre-designing electrolyte for specific organics was unfulfilled.

In this work, the dissolution issue of tricarbonyl compounds was addressed by highly-concentrated electrolyte. 5,7,12,14-Pentacenetetrone (PT) was chosen as the research object, as a typical member in quinone family, its molecular weight as well as molecular size was bigger than benzoquinone (BQ) and anthraquinone (AQ) (Scheme 1). Thus, the larger conjugate structure led to reduced dissolution in common electrolyte. More than that, the 4 active-site sharing by 5 aromatic nucleus conferred a capacity advantage over AQ (317 mAh/g vs. 257 mAh/g of AQ). However, significant capacity decay was usually observed on PT and stable long-term cycling was still a big challenge.[25–27] Highly-concentrated electrolyte was used to address the dissolution issue of PT. Besides, the underlying relationship between electrolyte and PT, and its evolution along with charging/discharging was investigated. Different electrolyte recipe was proposed toward the capacity-retention preference or power-density preference. The work not only supplies a strategy that contribute to the stable cycling, also provides some clues for electrolyte screening for specific organics.

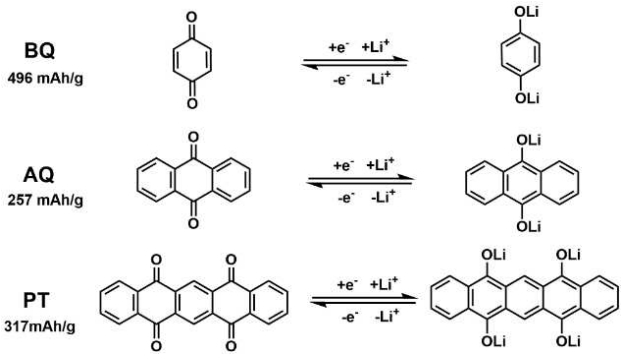

Scheme 1. Charge-discharge mechanism and theoretical specific capacity of BQ, AQ and PT.

Results and Discussion

PT has a pentaphenetetraketone structure, which can store and release charge through the conversion between ketone and enol structure (Scheme 1). It can deliver 317 mAh/g capacity if up to 4 electrons being injected. Though its larger conjugated molecule makes it less soluble than BQ and AQ, dissolution loss is still the main reason for its capacity decay. Previous study showed that using $[PY_{13}][TFSI]^-$ based Ionic liquid electrolyte much improved its cycling stability,[28] and special polymer separator also significantly suppressed the shuttle of dissolved organic species. but these approaches were not sufficient to support a long-run Li-PT organic cell. With these pioneer works, we tried to address the stability issue with the highly concentrated electrolyte.

Typical electrolyte was first examined, and they were 1 M $LiPF_6$ EC/DMC, 1 M LiTFSI DOL/DME. Severe capacity decay was observed in these two commercial electrolytes (Figure S1). In carbonate electrolyte, 298 mAh/g capacity was released by PT in the first cycle, very close to the theoretical value, but followed by quick and continuous capacity drop; in ether electrolyte, relatively lower initial capacity was obtained, and it only maintained for 2 cycles and then severe shuttle occurred. Carefully comparing the voltage profiles in Figure 1(a and b),

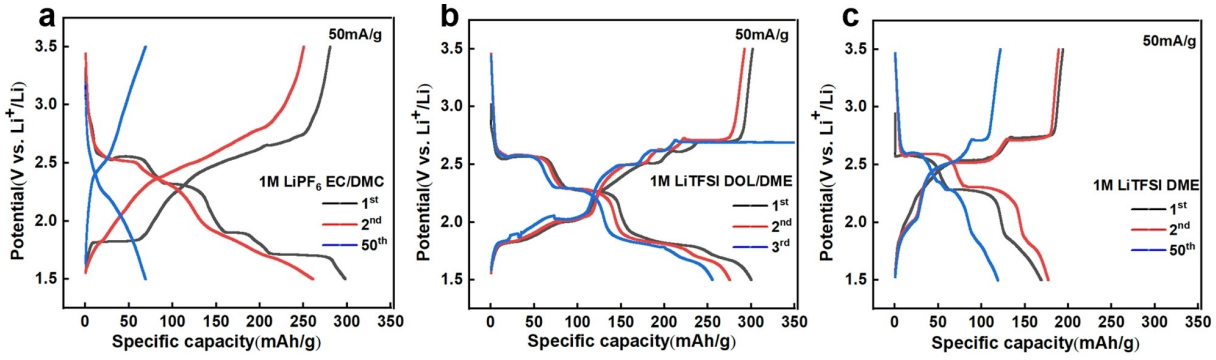

Figure 1. Galvanostatic charge-discharge curves of Li|PT cells in a) 1 M $LiPF_6$ EC/DMC, b) 1 M LiTFSI DOL/DME, and c) 1 M LiTFSI DME at the current density of 50 mA/g.

Research Article
doi.org/10.1002/batt.202200436
Chemistry Europe
European Chemical Societies Publishing

we noticed that either in 1 M $LiPF_6$ EC/DMC or 1 M LiTFSI DOL/DME, four discharging platforms was observed in the 1st discharging, corresponding to Li^+-association with four carbonyl groups. However, the 4-discharging-plateau characteristic was only preserved in 1 M LiTFSI DOL/DME, while in 1 M $LiPF_6$ EC/DMC, the well-distinguished plateau disappeared in the 1st charging and barely observed in the subsequent cycles. The dramatic change indicated the side-reaction between discharging product of PT and carbonate electrolyte. Actually, such phenomenon was observed previously though not clearly pointed out. The enolized discharged product of C–C=O was a good nucleophile, and it could attack the electrophilic carbonate solvent, especially the linear esters. The interaction was almost absent in N–C=O due to its enhanced stability. Thus, we saw polyimide was much less selective for electrolyte than quinones[29,30] and ether electrolyte was used in most quinone-based organics.

To investigate the origin of shuttle reaction, another electrolyte of 1 MLiTFSI DME was prepared. When PT cathode was tested in it, capacity decay was still observed (Figure 1c), namely, from 175 mAh/g in the 1st cycle to 134 mAh/g in the 50th cycle, but the shuttle reaction was significantly suppressed and distinct charging/discharging plateaus was continuously exhibited. The result suggested the prominent role of DOL in shuttle occurrence and it was further proved by the voltage profiles of PT in 1 M LiTFSI DOL (Figure S2a). The continuously decreasing efficiency in the initial three cycles indicated intensified shuttle along with cycling. In the dissolution experiment (PT electrode was immersed in DOL or DME) in Figure S2(b), we found PT immediately dissolved in DOL and the dark purple color implied more profound and yet unknown interaction between them. While in DME solvent, mild dissolution was observed. More importantly, though cycling stability was far from satisfactory, in 1 M LiTFSI DME, 4-electrons reaction of PT was achieved as being reflected by the 4 redox peaks in the CV plot (Figure S3a), additionally, reversible structure transformation between ketone and enol (Figure S3b) was realized accompanied with reversible crystal-structure change (Figure S3c). According to the preliminary screening, DME ether was chosen for further investigation.

We first tried to reduce the dissolution by increasing the electrolyte viscosity as this approach attained a measure of success in sulfur or other organic electrodes.[31,32] DME, G2, G3 and G4 could be viewed as glymes with repeating CH_2–O–CH_2 unit. When being used as single solvent in electrolyte, with the increasing of chain length, viscosity increased from 1.08 mPas of 1 M LiTFSI DME to 8.677 mPas of 1 M LiTFSI G4, accompany with obvious conductivity decreasing (12.7 to 3.08 mS/cm in Figure 2a). Figure 2(b) showed the effect of chain length on the cycling stability of PT. The result was unexpected that the increased viscosity did not bring improved stability, instead, worse capacity retention was obtained. For example, in 1 M LiTFSI G2 electrolyte, very high capacity of 314 mAh/g was released in the first cycle, but it decreased to 125 mAh/g after the 50th cycling, and quick capacity decay was also observed in the 1 M LiTFSI G3 electrolyte. It was even worse in 1 M LiTFSI G4, in which lower capacity and more severe capacity loss was obtained. The result indicated that the dissolution issue of PT could not be well addressed by simply increasing the chain length of ether, and it was confirmed by the dissolution test shown in Figure 2(c). Except in 1 M LiTFSI DME, fresh PT cathode (charged state) were readily dissolved in other three

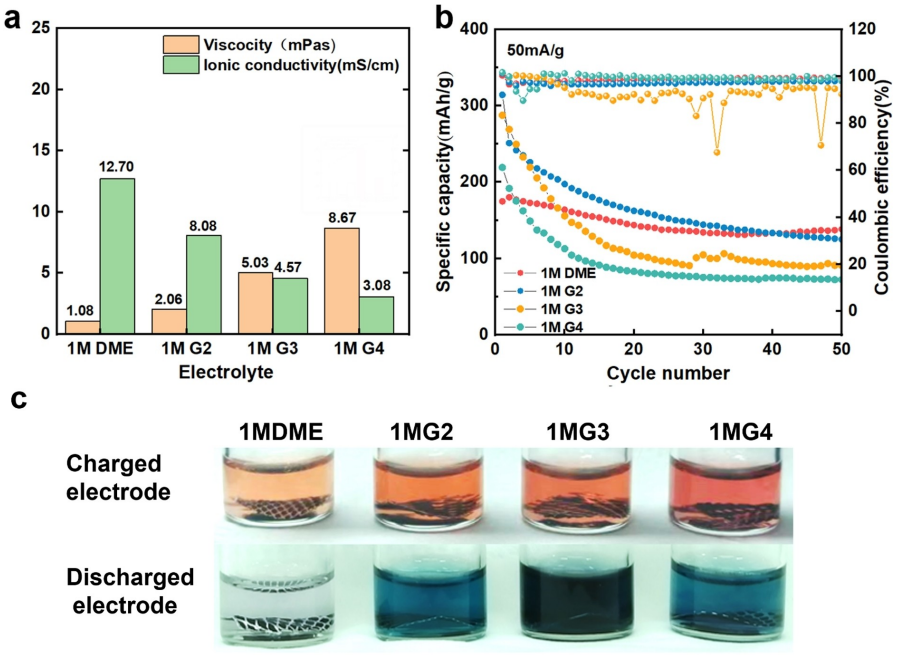

Figure 2. a) The viscosity, conductivity of 1 M LiTFSI DME, 1 M LiTFSI G2, 1 M LiTFSI G3, 1 M LiTFSI G4. b)The specific discharging capacity and Coulombic efficiency versus cycle numbers in these electrolytes at the current density of 50 mA/g. c) Solubility of charged and discharged PT electrodes in 1 M LiTFSI DME, 1 M LiTFSI G2, 1 M LiTFSI G3, 1 M LiTFSI G4 after 12 hours standing.

Research Article
doi.org/10.1002/batt.202200436
Chemistry Europe
European Chemical Societies Publishing

electrolytes, and similar phenomenon was observed on the discharged PT cathode. The phenomenon was consistent with the observation obtained on sulfur electrode which also presented deteriorated stability in G2, G3 and G4 than DME, and it was ascribed to the unclarified effect of DN value.[33]

We then tried to make concentrated electrolyte with different ether, with the expectation that ether solvent could be "immobilized" by electrolyte salt, and thus weakened the dissolving capacity toward PT or its discharging product. G4 was excluded due to its high viscosity. LiTFSI was very soluble in DME and G3, in which its maximum concentration was up to 8 M (Figure S4). We noticed that G3-containing electrolyte was visibly more viscous than DME-containing electrolyte. In contrast, the solubility in G2 was less than 2 M. The cycling test in Figure S5(a) indicated that increasing the concentration of LiTFSI in G2 did not bring obvious stability improvement. In Figure S5(b), we noticed that when G3 being the solvent, higher LiTFSI concentration could help to better preserve the capacity, but the smaller than 100% and wildly fluctuated efficiency in the mid/late-stage cycling suggested the shuttle occurrence. In the voltage profiles in Figure S5(c), we found severe shuttle reaction of PT cathode happened in 1 M LiTFSI G3, and it alleviated in a certain degree when the electrolyte salt concentration increased, but the shuttle issue still could not be well tackled even in 4 M LiTFSI G3.

The PT cathode was tested in 1–5 M LiTFSI DME electrolyte. In Figure 3(a), linear improvement of cycling stability was obtained with concertation increasing. For instance, from 1 M to 2 M, the capacity retention enhanced from 29% to 43% after 300 cycles. In 5 M LiTFSI DME, almost no significant capacity reduction was observed even after 500 cycles and more than 183 mAh/g capacity (91% of 201 mAh/g@1st) was stably released, such performance was first achieved on PT. The dissolution information of PT electrode was acquired by visual

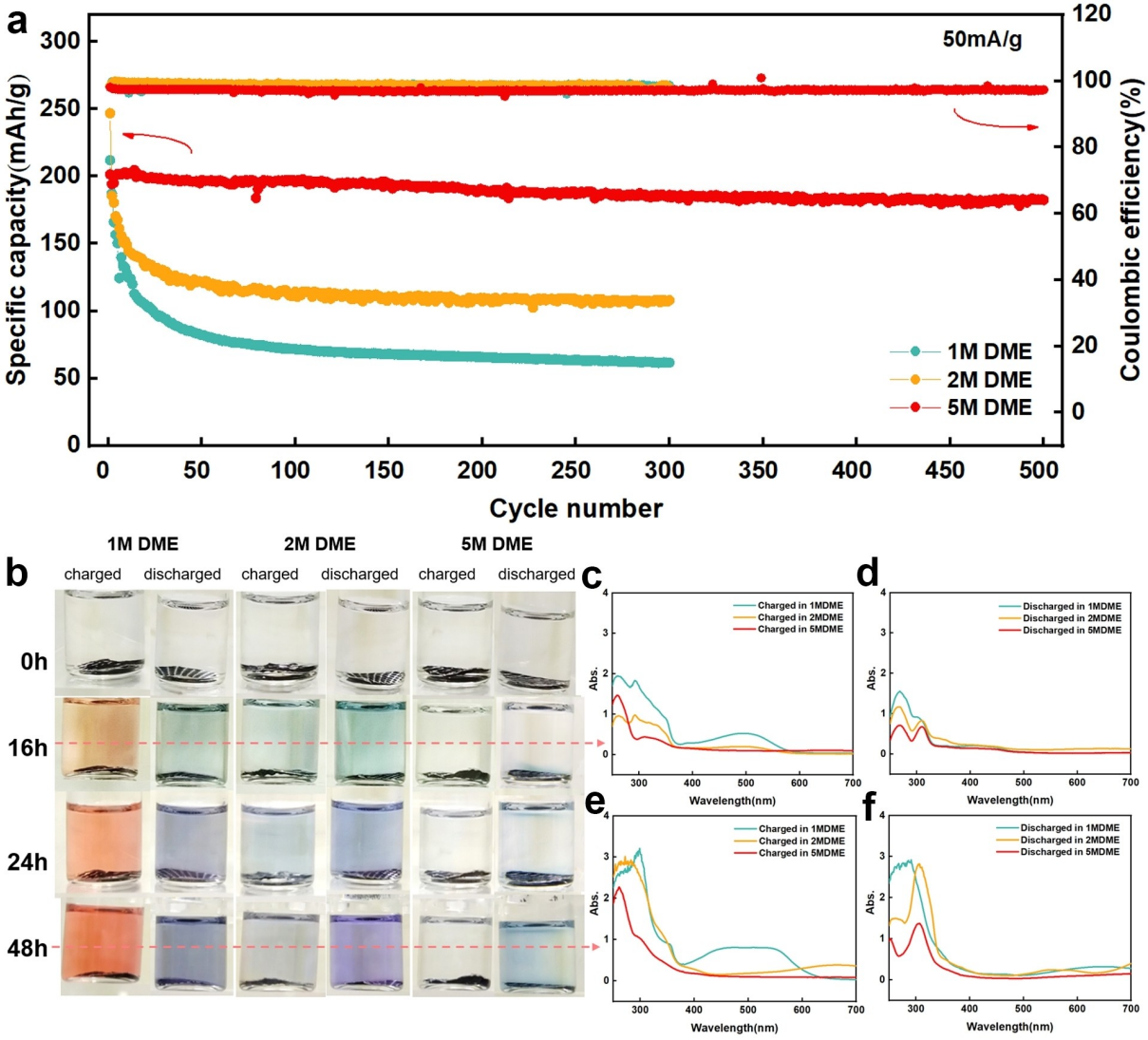

Figure 3. a) Long-cycle performance of PT electrode in 1 M LiTFSI DME, 2 M LiTFSI DME, 5 M LiTFSI DME. b) Visual observation of the dissolution of charged or discharged PT electrode in the three electrolytes. The UV-Vis spectrum of electrolyte in which charged/discharged PT electrode was immersed for c, d) 16 hours and e, f) 48 hours.

Research Article
doi.org/10.1002/batt.202200436
Chemistry Europe
European Chemical Societies Publishing

observation and UV test (The UV spectrum of LiTFSI or PT was supplied in Figure S6a for better comparison). Charged (pristine) or discharged PT electrode was immersed in electrolytes, and the electrolyte was intermittently extracted and subjected to UV measurement. We found that in 1 M LiTFSI DME, both charged and discharged PT electrode obviously dissolved after 16 hours immersion and it was witnessed by the color change of electrolyte (Figure 3b) as well as the characteristic UV-absorption in Figure 3(c and d). The dissolution was alleviated as being evidenced by the weaker UV-vis signals (it needs to be noted that the color change of electrolyte mostly depends on the amount of dissolved PT species, when immersing pristine PT electrode in 2 M LiTFSI DME for 7 days, the accumulation of the dissolving species changed the electrolyte in light-orange color, like that in 1 M LiTFSI DME after 16 hours-standing, thus color change rather than color darkness was the primary indicator of PT dissolution). In 5 M LiTFSI DME, the dissolution of charged PT was substantially prevented, even after 48 hours immersion, slight PT signal was found in the UV-spectrum (most of the absorption band could be ascribed to LiTFSI). Even for the discharged PT, least dissolution was obtained in 5 M LiTFSI DME, and notable dissolution could only be observed after 48 hours immersion. Thus, the best cycling stability of PT in 5 MLiTFSI DME could be explained by the much-suppressed dissolution loss. Additionally, increased viscosity also helped as the dissolved species could be confined within the cathode region rather than diffuse into electrolyte.

Figure 4(a) compared the voltage profiles of PT cathode. In 1 M LiTFSI DME, along with the cycling, the voltage hysteresis between the charging and discharging plateau was enlarged (Figure 4a), and impedance results showed the corresponding R_{CT} increase (Figure 4d and Table S2). The polarization increment was reduced in 2 M LiTFSI DME (Figure 4b and e), and further completely suppressed in 5 M LiTFSI DME (Figure 4c) where very stable R_{CT} value was maintained even after 100 cycles (Figure 4f). The evolvement of the voltage profiles and polarization in different electrolytes was highly related to the dissolution. With the dissolving species entering into electrolyte, the contact between conductive carbon and active material was damaged, and it was reflected by the increased polarization and R_{CT} value.

The degraded contact was proved by SEM observation. After the 1st charging in 1 M LiTFSI DME (Figure 5a), cracks and holes were found on PT electrode. Besides, the strip-like deposits indicated the recrystallization of PT and it was also confirmed by the EDS-mapping in Figure S7 and shaper XRD peaks (usually more narrow diffraction peak indicates higher crystallinity and bigger grain size) in Figure S8. However, after the 100th charging, the strip-like deposits no longer appeared, and big-or-small holes scatted on the electrode surface along with many cracks (Figure 5d). Meanwhile, in the XRD pattern, characteristic PT peaks mostly disappeared, only few widened and weakened XRD peaks were preserved, suggesting the much-reduced particle size. Similar change was observed in 2 M LiTFSI DME (Figure 5b and e). In 5 M LiTFSI DME, the case was quite different. The electrode integrity was well maintained (Figure 5c and f). After 100 cycles, we also found the stripe-like deposition on electrode surface, implying the occurrence of dissolution, but due to the very limited solubility of PT or its discharging product in 5 M LiTFSI DME, the particle dimension

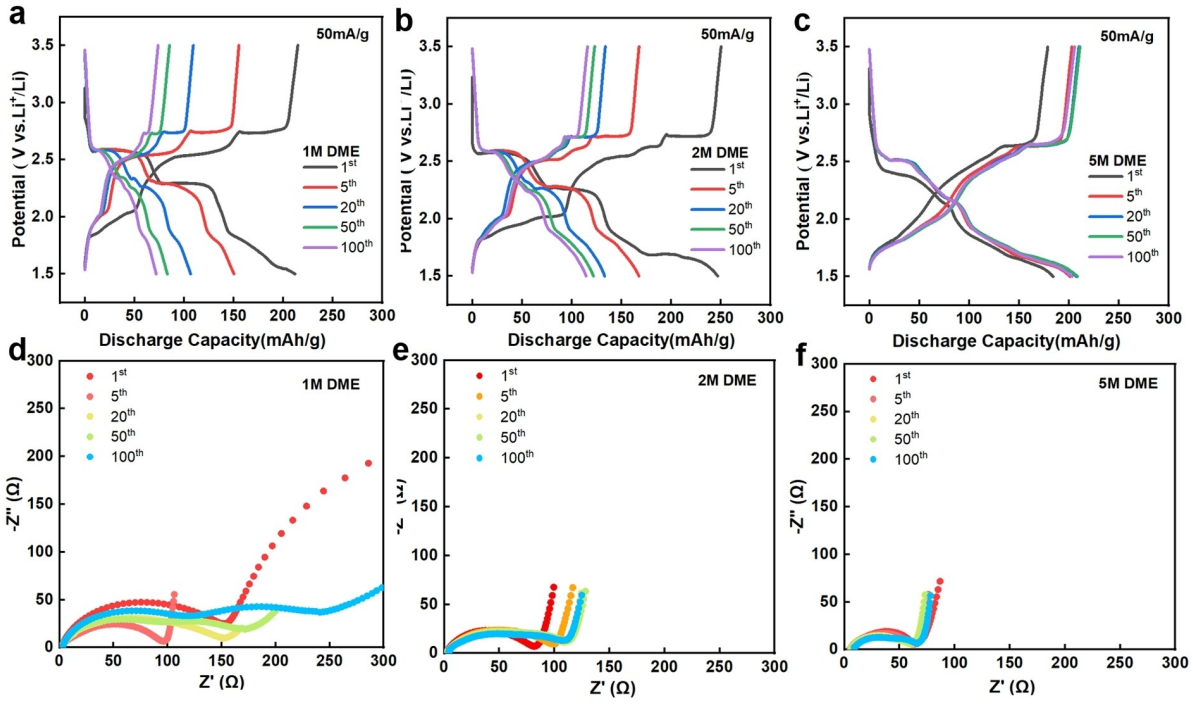

Figure 4. Voltage profiles and electrochemical impedances collected after 1st, 5th, 20th, 50th, and 100th cycles in a and d) 1 M LiTFSI DME, b and e) 2 M LiTFSI DME, and c and f) 5 M LiTFSI DME.

Research Article
doi.org/10.1002/batt.202200436
Chemistry Europe
European Chemical Societies Publishing

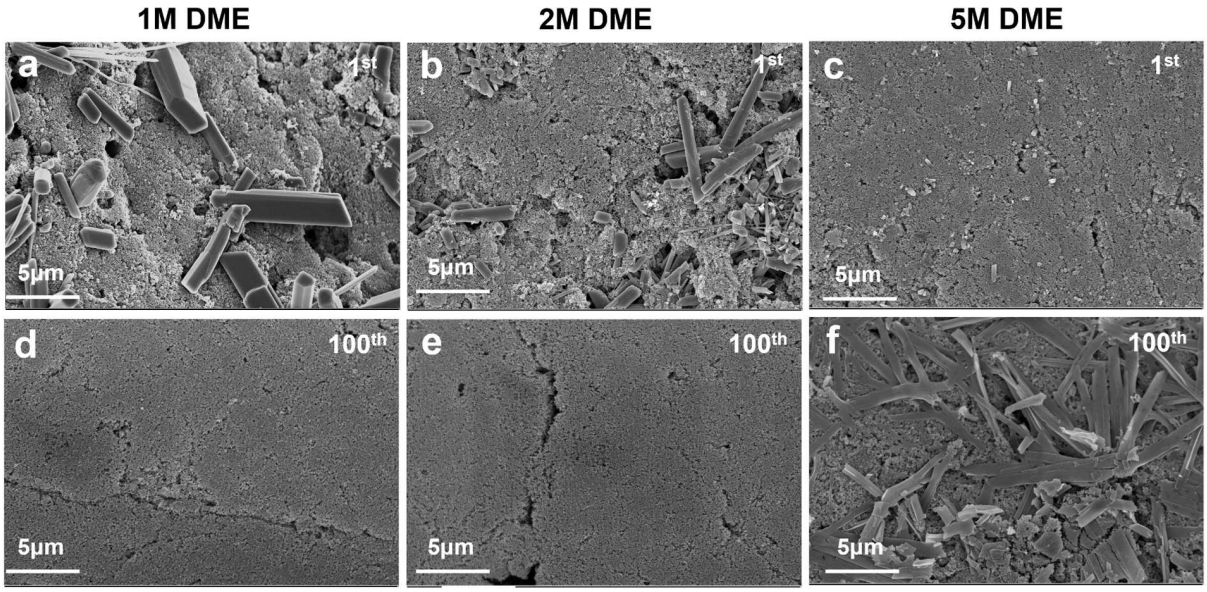

Figure 5. SEM images of the electrodes after cycling in a and d) 1 M LiTFSI DME, b and e) 2 M LiTFSI DME, and c and f) 5 M LiTFSI DME for one cycle and 100 cycles.

remained mostly unchanged as being reflected by the as sharp XRD peaks in Figure S8.

In the above, highly concentrated electrolyte was found to well resolve the dissolution loss of PT electrode, however, it cannot be ignored that concentrated electrolyte has rather high viscosity which may bring poor electrode infiltration. Actually, we also have to admit that even in such concentrated electrolyte, PT dissolution was not completely prevented, thus if the PT cathode is required to run for a long time and work with unplanned intervals, using 5 M LiTFSI DME may not be a reliable solution. Besides, the guiding rule for choosing optimum electrolyte for PT is unclarified. Thus, further investigation was conducted towards these issues.

In Figure S9(a), the very slow spreading of 5 M LiTFSI DME on separator witnessed the poor infiltration of concentrated electrolyte. Taking this into account, 20% hexane or THF was added in 5 M LiTFSI DME with the aim of reducing viscosity. With their adding, the real concentration of LiTFSI decreased accordingly. The viscosity obviously decreased as being expected (Figure 6a) and improved electrode/separator infiltration was also observed (Figure S9b and c). Accompany with it, the conductivity changed in different degree. We found that THF-adding could most decreased the viscosity and it also enhanced the conductivity by twice. While hexane adding could decreased the viscosity by half, and the conductivity mostly remained unchanged. The result was consistent with the polarity of solvent. THF and DME (or analogues glymes) has similar dielectric constant, they both are polar solvent, on the contrary, hexane is typical non-polar solvent. Thus, THF or DME could help the Li^+ solvation while hexane was inert and its adding could only reduce the viscosity. To better understand the polarity of mixed solvent, $E_T(30)$ empirical parameter[34–36] of DME + hexane or DME + THF(the volume ratio was as same as that in 5 M LiTFSI DME + 20% hexane/20%THF) was obtained

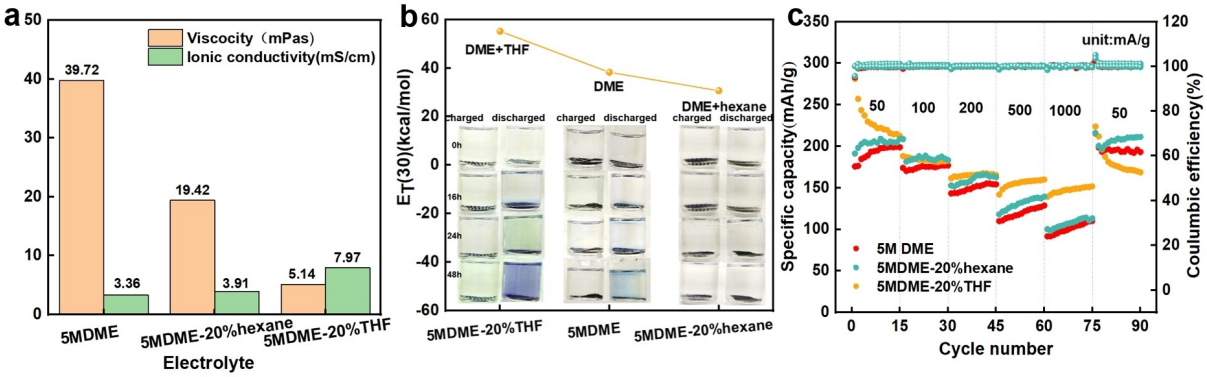

Figure 6. a) The viscosity, conductivity of 5 M LiTFSI DME, 5 M LiTFSI DME-20% hexane, 5 M LiTFSI DME-20% THF, b) Visual observation of the dissolution of charged or discharged PT electrode in three different electrolytes (the immersion time was 24 hours) and $E_T(30)$ values of DME, DME + THF and DME + hexane solvent. c) Rate performance of PT in 5 M LiTFSI DME, 5 M LiTFSI DME-20% hexane, 5 M LiTFSI DME-20% THF.

and compared with DME. In Figure 6(b), we noticed that DME mixing with THF brought higher $E_T(30)$, implying increased polarity; while DME + hexane mixture presented lower $E_T(30)$. Although in 5 M LiTFSI DME or 5 M LiTFSI DME + 20% hexane(THF) electrolyte, the coordination between Li^+ and solvent complicated the real solvent environment, the comparison of $E_T(30)$ still supplied a helpful clue from which we can roughly estimate the dissolution of PT (or discharging product). According to "like dissolves likes" principle, adjusting the polarity of electrolyte could be an effective approach to alleviate the dissolution of PT. PT is intrinsically low-polar due to its symmetrical molecular structure, with the discharging processing, its polarity increases with O–Li formation, thus if non-polar solvent is used, the dissolution of PT can be substantially avoided. Although non-polar solvent is infeasible because of the ion-transfer requirement of electrolyte, the rule of "the weaker polarity of the solvent, the less dissolution of PT" can help us to quickly pick up the matched electrolyte. Actually, if revisiting the cycling result shown in Figure 2(b), such rule could also be attested as DME has the lowest $E_T(30)$, correspondingly weakest polarity among the glymes. Therefore, in Figure 6(b), we saw that if comparing with 5 M LiTFSI DME, THF-adding brought higher polarity, hence increased dissolution; while hexane-adding decreased the polarity and the dissolution as well. The LSV tests in Figure S10 indicated that both 5 M LiTFSI DME and 5 M LiTFSI DME + 20% hexane/20% THF had sufficient electrochemical window for Li/PT cell, as they all exhibited appreciable anodic current when the voltage was higher than 5 V vs. Li^+/Li.

We further examined the effect of co-solvent on the electrochemical property of PT. In Figure S11, when using 5 M LiTFSI DME-20%THF electrolyte, bigger capacity decay was observed than 5 M LiTFSI DME, in accord with the higher polarity of DME + THF and more obvious PT dissolution, but it led to notably improved rate capacity of PT (Figure 6c). When the current increased from 50 mA/g to 1000 mA/g, 66.5% capacity was preserved, much higher than that obtained in 5 M LiTFSI DME. Comparatively, 5 M LiTFSI DME-20%hexane significantly reduced the PT dissolution, it consequently brought better capacity retention, but the improvement in rate capability was rather limited if comparing with 5 M LiTFSI DME-20%THF.

To better understand the effect of co-solvent on the interface chemistry or surface morphology, Li anode or PT cathode was taken out from the Li/PT cells that had been cycled one time, and then they were well washed and subjected to SEM or XPS characterization. The surface morphology of PT cathodes cycled in 5 M LiTFSI DME or 5 M LiTFSI DME + 20%hexane electrolyte was quite similar (Figure S12), but when THF being added, the strip-like deposits was found, similar to that observed in 1 M LiTFSI DME or 2 M LiTFSI DME (Figure 5a and b), indicating the occurrence of dissolution and re-crystallization of PT. The comparison of SEM images collected on Li anodes indicated that when using 5 M LiTFSI DME or 5 M LiTFSI DME + 20%hexane electrolyte, the deposited Li presented block-like morphology, and in the latter electrolyte, the Li-deposition was denser; while using 5 M DME + 20% THF electrolyte, bar-like deposition and much smaller particle size was observed on Li anode (Figure S12). The difference might be explained by the different Li-deposition kinetic induced by the diffent solvent and different SEI property.

In Figure S13, we noticed that using different electrolyte did not bring significant difference in the XPS spectra of PT cathodes, all the XPS signals could be ascribed to PT reduction/re-oxidation products and electrolyte species. However, THF-adding led to dramatically decreased C–F band. The result could be explained by the polar-character of THF. Unlike hexane, THF could be involved in Li^+-solvation, thus when THF was added in 5 M LiTFSI DME, the electrolyte environment could be greatly changed, the original Li^+-DME coordination might be replaced by Li+-DME/THF coordination accompany with the change in Li^+-solvation structure, hence solvent decomposition rather than salt decomposition dominated the SEI species, leading to the obvious reduction of C–F signals that was originated from the electrolyte salt.

Now through adjusting the polarity of electrolyte, we designed two kinds of electrolytes for PT electrode, 5 M LiTFSI DME-20%n-hexane could substantially eliminate the dissolution loss and was expected to well support the long-running of PT; on the other hand, if power performance was preferred, 5 M LiTFSI DME-20%THF could be a good candidate, PT presented comparable stability in it as in 5 M LiTFSI DME, and the rate performance was greatly boosted. The two electrolyte both effectively reduced the viscosity. In addition, according to "like dissolve like", a guided rule could be proposed that non-polar solvent and thus-prepared electrolyte could completely solve the dissolution issue of PT or its analogues. However, it has to be pointed out that, in this study, (PT) cathode is the main research object, when practical battery is designed, the requirement from electrolyte and even counter electrode must be considered. Non-polar solvent, though can best tackle the dissolution issue, its poor dissolving capability as well as the possible incompatibility with anode and even the infiltration in the high-loading electrode must be considered. A practicable electrolyte must include the optimum composition of differently functioned solvent with viscosity, polarity and even DN(AN) values merits. Thus, many more efforts are still required to realize the application of PT organics or its analogues.

Conclusion

In this work, we tried to address the dissolution issue of PT organic electrode. Highly concentrated electrolyte of 5 M LiTFSI DME was used and it significantly reduced the dissolution and well maintained the capacity for 500 cycles long. The relationship between solvent/electrolyte property and dissolution, and the interaction between charged/discharged PT and electrolyte was investigated. A guiding rule of the dependence of dissolution on polarity was proposed. With the rule, non-polar solvent of hexane was further added to substantially eliminated the dissolution loss and reduce the electrolyte viscosity. The work not only tackled the dissolution issue of PT, it also

revealed the dominant factor in dissolution loss and supplied a common rule for electrolyte screening for organic electrode.

Experimental Section

Material preparations. 5,7,12,14-Pentacenetetrone (PT, 95%, TCI) was commercially purchased and directly used as received without further purification. Ether electrolytes were prepared in an argon-filled glove box by dissolving corresponding amount of lithium bis(trifluoromethanesulphonyl)imide (LiTFSI, 99.8%, Duoduo) into different ether solvent of 1,2-dimethoxyethane (DME, 99.5%, J&K scientific), bis(2-methoxy ethyl)ether(G2, 99%, J&K scientific), 1,1-Di(2-methoxy ethoxy)ethane (G3, 99%, J&K scientific), and Tetraethylene glycol dimethyl ether (G4, 98%, J&K scientific). Other solvent of Tetrahydrofuran (THF, 99.9%, adamas) and hexane (99.5%, J&K scientific) was added to highly-concentrated electrolyte, the information of solvents could be found in Table S1. Carbonate electrolyte was made by dissolving $LiPF_6$ in EC + DMC mixture solvent (1 : 1 v/v).

Cell fabrication. The PT cathodes were made by mixing 60 wt% PT, 30 wt% KB carbon (Ketjen black EC-600JD) and 10 wt% polytetrafluoretyhylene (PTFE, 10% aqueous solution, Canrd) binder, and pressing the well-blended mixture onto an Al-mesh current collector. The area of PT cathodes was 0.6 cm^2, and the mass loading of PT was 1.5 ± 0.2 mg/cm^2. The CR2016 type cells were assembled in an argon-filled glove box, and lithium foil was the anode, Celgard 2500 was the separator. 60 μL electrolyte was added in each cell.

Electrochemical tests. The galvanostatic charge/discharge tests were conducted on a LANHE CT2001 A battery test system (Wuhan, China) with a current density of 50 mA/g and a voltage range of 1.5 V–3.5 V vs. Li^+/Li unless specified. The cyclic voltammetry (CV) was carried out on CHI600 A electrochemical workstation, the voltage window was 1.5–3.5 V. Electrochemical impedance spectroscopy (EIS) was obtained on Autolab Electrochemical Workstation (Eco Chemie). The test frequency range was 0.1–10^6 Hz, and the voltage amplitude was 10 m V. All the electrochemical tests were conducted at 30 °C.

Characterizations of electrolyte. The ionic conductivity of electrolytes was measured on Reichi DDB 303a conductometer (Shanghai, China) at room temperature. The Viscosity was measured by Ubbelohde Viscometer (Jiangsu, China). The polarity of solvent was determined by $E_T(30)$ method.[37] Precisely quantified Reichardt's dye (90%, Sigma-Aldrich) was dissolved in 1 ml solvent, and UV-VIS test (UV-3600,SHIMADZU, Japan) was performed. The empirical parameter of $E_T(30)$, reflecting the polarity, was determined by the equations in SI.

Other characterizations. IR measurement was conducted on discharged electrode. The cell was disassembled after the 1st discharging, and PT cathode was taken out, washed with DME for 2–3 times and dried, then it was subjected to IR measurement (ALPHA ii infrared spectrometer, Bruker Germany). The dissolution of discharged PT was traced by UV-visible spectrophotometry. After the 1st discharging, PT cathode was taken out, washed with DME to remove the surface residue, and immersed in 2 mL corresponding electrolyte. After standing for different time, UV-visible measurements (UV-3600, SHIMADZU, Japan) were conducted within a wavelength range of 250–700 nm. The crystalline structure of charged and discharged PT electrode was determined in term of X-ray diffraction (Cu Kα, 10° to 50°, MiniFlex 600 X-ray diffraction, Rigaku, Japan). The morphology of PT electrodes was observed with MERLIN Compact scanning electron microscope (Zesis, Germany). It should be noted that all samples were well-sealed to avoid air exposure during the sample transfer.

Acknowledgements

We gratefully acknowledge the financial support from the National Natural Science Foundation of China (No. 21875172) and 210900038).

Conflict of Interest

The authors declare no conflict of interest.

Data Availability Statement

The data that support the findings of this study are available on request from the corresponding author. The data are not publicly available due to privacy or ethical restrictions.

Keywords: dissolution loss · electrochemistry · organic electrode material · polarity · quinones

[1] M. Armand, J. M. Tarascon, *Nature* **2008**, *451*, 652–657
[2] C. Liu, Z. G. Neale, G. Cao, *Mater. Today* **2016**, *19*, 109–123
[3] F. Schipper, D. Aurbach, *Russ. J. Electrochem.* **2016**, *52*,1095–1121
[4] Z. P. Song, H. S. Zhou, *Energy Environ. Sci.* **2013**, *6*, 2280–2301
[5] T. B. Schon, B. T. McAllister, P. F. Li, D. S. Seferos, *Chem. Soc. Rev.* **2016**, *45*, 6345–6404
[6] Y. Lu, Q. Zhang, L. Li, Z. Niu, J. Chen, *Chem.* **2018**, *4*, 2786–2813
[7] Y. Lu, J. Chen, *Nat. Chem. Rev.* **2020**, *4*, 127–142
[8] H. Chen, M. Armand, G. Demailly, F. Dolhem, P. Poizot, J. M. Tarascon, *ChemSusChem* **2008**, *1*, 348–355
[9] B. Yan, L. Wang, W. Huang, S. Zheng, P. Hu, Y. Du, *Inorg. Chem. Front.* **2019**, *6*, 1977–1985
[10] H. M. Sun, B. Yang, W. W. Huang, L. Q. Wang, *Energy Storage Sci. Technol.* **2019**, *8*, 702
[11] Z. P. Song, H. Zhan, Y. H. Zhou, *Chem. Commun.* **2009**, *4*, 448–450
[12] F. Benjamin, J. Badr, A. Mohamed, A. Mérièm, *Mater Adv* **2021**, *2*, 376–383
[13] J. Yang, Z. P. Wang, Y. Q. Shi, P. F. Sun, Y. H. Xu, *ACS Appl. Mater. Interfaces* **2020**, *12*, 7179–7185
[14] M. Yao, K. Kuratani, T. Kojima, N. Takeichi, H. Senoh, T. Kiyobayashi, *Sci. Rep.* **2014**, *4*, 1–6
[15] M. Lee, J. Hong, H. Kim, H. D. Lim, S. B. Cho, K. Kang, C. B. Park, *Adv. Mater.* **2014**, *26*, 2558–2565
[16] J. Lee, H. Kim, M. J. Park, *Chem. Mater.* **2016**, *28*, 2408–2416
[17] M. R. Tuttle, S. Y. Zhang, *Chem. Mater.* **2019**, *32*, 255–261
[18] Z. G. Chen, J. Wang, T. Cai, Z. Hu, J. Chu, F. Wang, Z. Song, *ACS Appl. Mater. Interfaces* **2022**, *14*, 27994–28003
[19] M. R. Tuttle, S. T. Davis, S. Y. Zhang, *ACS Energy Lett.* **2021**, *6*, 643–649
[20] L. Sieuw, A. Jouhara, É. Quarez, C. Auger, J. F. Gohy, P. Poizot, A. Vlad, *Chem. Sci.* **2019**, *10*, 418–426
[21] T. Xu, J. Qin, Y. Liu, Q. Lan, Y. Zhao, Z. P. Song, H. Zhan, *ChemElectroChem* **2021**, *8*, 4625–4632
[22] T. Cai, Y. Han, Q. Lan, F. Wang, J. Chu, H. Zhan, Z. P. Song, *Energy Storage Mater.* **2020**, *31*, 318–327
[23] Z. Q. Zhu, M. L. Hong, D. S. Guo, J. F. Shi, Z. L. Tao, J. Chen, *J. Am. Chem.* **2014**, *136*, 16461–16464
[24] M. G. Li, J. X. Yang, Y. Q. Shi, Z. F. Chen, P. X. Bai, H. Su, P. X. Xiong, M. G. Cheng, J. W. Zhao, Y. H. Xu, *Adv. Mater.* **2022**, *34*, 2107226
[25] M. Yao, H. Senoh, T. Sakai, T. Kiyobayash, *Int. J. Electrochem. Sci.* **2011**, *6*, 2905–2911

[26] Y. Fang, C. Chen, J. Fan, M. Zhang, W. Yuan, L. Li, *Chem. Commun.* **2019**, *55*, 8333–8336
[27] S. Zhu, M. Tang, Y. Wu, Y. Chen, C. Jiang, C. Xia, S. Zhuo, B. Wang, C. Wang, *Sustain. Energy Fuels* **2019**, *3*, 142–147
[28] H. Sun, W. Zhou, W. Huang, L. Wang, *Chin. J. Inorg. Chem.* **2020**, *36*, 1701–1706
[29] A. E. Lakraychi, K. Fahsi, L. Aymard, P. Poizot, F. Dolhemad, J. P. Bonnet, *Electrochem. Commun.* **2017**, *76*, 47–50
[30] J. Aher, A. Graefenstein, G. Deshmukh, K. Subramani, B. Krueger, M. Haensch, J. Schwenzel, K. Krishnamoorthy, G. Wittstock, *ChemElectroChem* **2020**, *7*, 1160–1165
[31] Z. Jiang, Z. Zeng, W. Hu, Z. Han, S. Cheng, J. Xie, *Energy Storage Mater.* **2021**, *36*, 333–340
[32] Y. Peng, R. Badam, T. Jayakumar, W. Wannapakdee, *J. Electrochem. Soc.* **2022**, *169*, 050515
[33] Y. Yuan, F. R. Qin, K. Zhang, Y. Q. Lai, Y. X. Liu, *Chin. J. Nonferrous Met.* **2016**, *26*, 1473–1479
[34] M. J. Muldoon, C. M. Gordon, I. R. Dunkin, *J. Chem. Soc. Perkin Trans. 2* **2001**, *4*, 433–435
[35] S. P. Zanotto, M. Scremin, C. Machado, M. C. Rezende, *J. Phys. Org. Chem.* **1993**, *6*, 637–641
[36] P. M. E. Mancini, A. Terenzani, M. G. Gasparri, L. R. Vottero, *J. Phys. Org. Chem.* **1995**, *8*, 617–625
[37] V. G. Machado, C. Machado, *J. Chem. Educ.* **2001**, *78*, 649

Revised manuscript received: November 8, 2022
Version of record online: November 24, 2022